PREPARED FOR THE U.S. DEPARTMENT OF ENERGY,
UNDER CONTRACT DE-AC02-76CH03073

PPPL-3893
UC-70

PPPL-3893

Next-step Spherical Torus Experiment and Spherical Torus Strategy in the Fusion Energy Development Path

by

M. Ono, M. Peng, C. Kessel, C. Neumeyer, J. Schmidt, J. Chrzanowski, D. Darrow, L. Grisham, P. Heitzenroeder, T. Jarboe, C. Jun, S. Kaye, J. Menard, R. Raman, T. Stevenson, M. Viola, J. Wilson, R. Woolley, and I. Zatz

October 2003

PPPL
PRINCETON PLASMA
PHYSICS LABORATORY

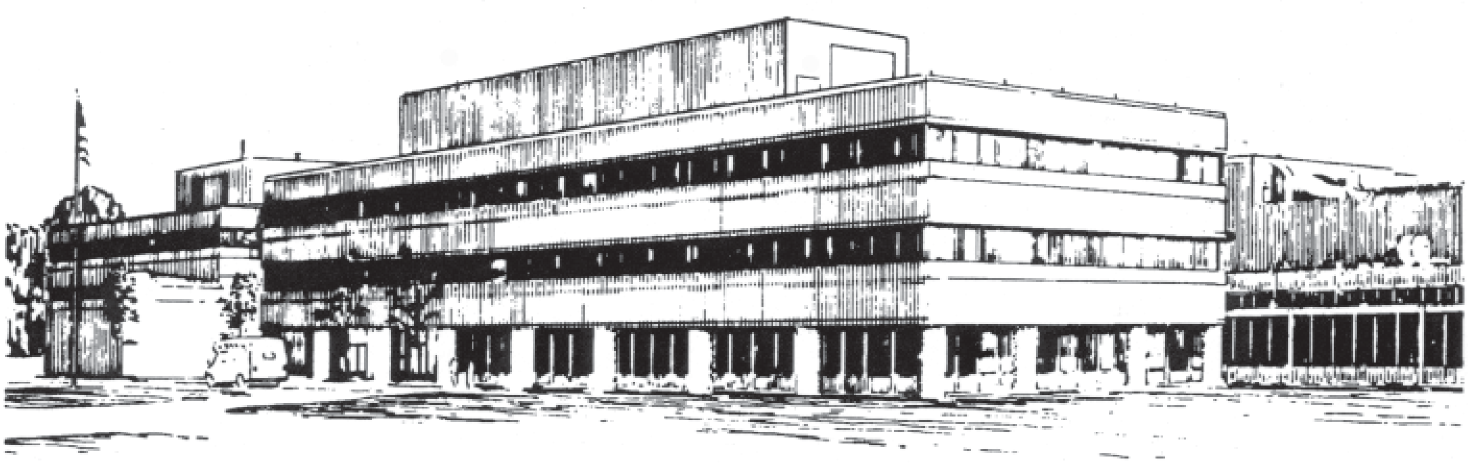

PRINCETON PLASMA PHYSICS LABORATORY
PRINCETON UNIVERSITY, PRINCETON, NEW JERSEY

PPPL Reports Disclaimer

Availability

This report is posted on the U.S. Department of Energy's Princeton Plasma Physics Laboratory Publications and Reports web site in Fiscal Year 2004. The home page for PPPL Reports and Publications is: http://www.pppl.gov/pub_report/

DOE and DOE Contractors can obtain copies of this report from:

U.S. Department of Energy
Office of Scientific and Technical Information
DOE Technical Information Services (DTIS)
P.O. Box 62
Oak Ridge, TN 37831

Telephone: (865) 576-8401

Fax: (865) 576-5728

Email: reports@adonis.osti.gov

This report is available to the general public from:

National Technical Information Service
U.S. Department of Commerce
5285 Port Royal Road
Springfield, VA 22161

Telephone: 1-800-553-6847 or
(703) 605-6000

Fax: (703) 321-8547

Internet: http://www.ntis.gov/ordering.htm

Next-Step Spherical Torus Experiment and Spherical Torus Strategy in the Fusion Energy Development Path

M. Ono 1), M. Peng 2), C. Kessel 1), C. Neumeyer 1), J. Schmidt 1), J. Chrzanowski 1), D. Darrow 1), L. Grisham 1), P. Heitzenroeder 1), T. Jarboe 3), C. Jun 1), S. Kaye 1), J. Menard 1), R. Raman 3), T. Stevenson 1), M. Viola 1), J. Wilson 1), R. Woolley 1), I Zatz 1)

1) Princeton Plasma Physics Laboratory, Princeton, NJ, USA

2) Oak Ridge National Laboratory, Oak Ridge, TN, USA,

3) University of Washington, Seattle, WA, USA

e-mail contact of main author: mono@pppl.gov, 52.55.Fd, 28.52.Av, 52.25.Xz

Abstract. A spherical torus (ST) fusion energy development path which is complementary to proposed tokamak burning plasma experiments such as ITER is described. The ST strategy focuses on a compact Component Test Facility (CTF) and higher performance advanced regimes leading to more attractive Demo and Power Plant scale reactors. To provide the physics basis for the CTF an intermediate step needs to be taken which we refer to as the "Next Step Spherical Torus" (NSST) device and examine in some detail herein. NSST is a "performance extension" (PE) stage ST with the plasma current of 5 - 10 MA, R = 1.5 m, and $B_T \leq 2.7$ T with flexible physics capability. The mission of NSST is to 1) Provide a sufficient physics basis for the design of CTF, 2) Explore advanced operating scenarios with high bootstrap current fraction / high performance regimes, which can then be utilized by CTF, DEMO, and Power Plants, and 3) Contribute to the general plasma / fusion science of high β toroidal plasmas. The NSST facility is designed to utilize the TFTR (or similar) site to minimize the cost and time required for the design and construction.

1. Spherical Torus Contributions Toward Fusion Energy Development Path

The potential of the Spherical Torus (ST) configuration to enable attractive fusion energy was discussed in a number of recent papers [1-3]. The engineering feasibility of a single-turn center leg for the toroidal field coils was identified as a key element for attractive ST reactors [1]. It should be noted that for spherical torus plasmas the plasma current and the toroidal field coil current are comparable, thus making the single-turn TF concept practical. The single turn design avoids the use of insulators in the center column, which in turn greatly reduces the shielding requirements. This type of simple TF center column leads to a very compact Component Test Facility (CTF) (sometimes referred to as the Volume Neutron Source (VNS)) with R ~ 1 - 1.5 m [2,3] assuming standard ST physics performance (such as β_T ~ 15 - 25%) to produce substantial neutron wall loading (W_L ~ 1 MW/m^2 or higher) at a modest total fusion power (~ 50 MW or higher). The mission of CTF would be to conduct testing and development of reliable high performance fusion nuclear components [4] for an attractive Demo power plant. Key assumptions are that, in order to realize a compact CTF with minimal inboard shielding, the center column cannot contain an ohmic solenoid and cannot utilize insulating materials as would be required for any multi-turn TF or OH coil. The solenoid-less plasma start-up demonstrated at the multi-MA level is therefore an important physics mission of the Next-Step Spherical Torus (NSST) experiment as described in this manuscript. Finally, we note that the minimization of the total fusion power (thus the tritium usage) is an important consideration for a CTF facility due to the limited availability of the tritium fuel estimated in the coming decades.

The criticality of CTF in the accelerated development of fusion energy was recently recognized more broadly in the U.S. fusion research community. For example, the preliminary report of the Fusion Development Path Panel under the US Fusion Energy Science Advisory Committee [5] states that "within the MFE (magnetic fusion energy) path, a significant experience is anticipated from testing plasma support technologies (e.g., superconducting magnets and plasma heating) in ITER. However testing of chamber technology in ITER is limited by the relatively low plasma duty cycle and the lower flux neutron fluence than encountered in Demo. Thus a Component Test Facility (CTF) is judged to be necessary in addition to a burning plasma experiment in order for Demo to meet its goals for tritium self-sufficiency, and practical, safe, and reliable engineering operation with high thermodynamic efficiency, rapid remote maintenance and high availability." The report further notes that "since the Demo is to demonstrate the operation of an attractive fusion system, it must not itself devoted to testing components for the first time in a fully realistic fusion environment. Furthermore the tritium consumption of a large facility such as Demo makes it impractical for developing tritium breeding components, as only very little operation without full breeding would be possible." One can therefore envision that a CTF facility would begin the operation at the level of neutron wall loading W_L ~ 1- 2 MW/m^2, and progressively upgrade the test components to handle higher W_L while improving ST plasma performance with the physics input from NSST. The CTF device is therefore expected to satisfy stringent operational requirements [3], such as complete modularity of all fusion core components (including the single-turn center leg) to permit rapid change out for replacement under fully remote conditions. The CTF device should also achieve the high neutron fluence (~6 MW-yr/m^2 or higher) required in the testing program.

The significant tritium consumption required for component testing puts a premium on compact devices that maximize W_L while minimizing the total fusion power. Due to the limited supply of tritium anticipated for the next few decades, net tritium consumption by CTF must be carefully managed. Towards this end the fusion neutrons lost to the center leg should to be minimized while maximizing the tritium capture and breeding ratios of the outboard blanket components. This consideration tends to drive the CTF design toward lower aspect ratio [1]. Such a compact CTF with high fusion and external drive powers is expected to lead to very high plasma heat and particle fluxes on the plasma facing components. Development of reliable high performance fusion blanket modules and plasma facing components (PFCs) under fusion nuclear conditions to aid an attractive DEMO design will therefore be an overarching goal of the CTF program.

An effective and accelerated development of fusion energy using key contributions from the ST can therefore be envisioned as shown in Fig. 1. Schematics of three representative ST devices, NSTX, NSST, and a version of CTF, are shown in Fig. 2. In Table 1, some key parameters for these three devices are listed. As illustrated in Fig. 1, the ST development path starts with the on-going Proof of Principle (PoP) level ST experiments (e.g., NSTX, MAST) to establish the physics principles of the ST concept at the Ip ≈ 1 MA level. A Performance Extension (PE) level ST experiment (NSST) with Ip = 5- 10 MA is needed to provide the ST physics database at fusion plasma parameters, including burning plasmas with potentially high Q values (≥ 2). Early in its operations, NSST will develop physics basis needed to design and construct a compact CTF device without an ohmic solenoid. This includes a demonstration of multi-MA solenoid-free start-up and non-inductive sustainment. Once the CTF physics feasibility demonstration is achieved on NSST, the CTF engineering design and construction can proceed at a separate nuclear site. The NSST facility can then continue to explore more advanced ST regimes to raise the plasma performance in CTF and help optimize the design of Demo. The initial CTF fusion blanket and other core components can utilize the ITER core technology and component designs, and benefit from the materials developed by IFMIF. The ST development path via CTF would therefore complements the tokamak burning plasma experiments such as ITER and the material testing facility such as IFMIF in order to optimize the Demo design.

As indicated in Table 1, the plasma and device parameters increase significantly, nearly an order of magnitude, from the existing 1 MA class devices represented by NSTX and MAST to the 10 MA class NSST. However, being a physics-oriented facility, the design philosophy of NSST is quite similar to that of NSTX and MAST, namely to maximize the device physics capabilities (physics tools as well as ample diagnostic access) with an effective use of existing site credits to minimize construction cost and time. On the other hand, while the plasma parameters are similar to NSST, the CTF facility is designed with the mission of testing and developing advanced core components for Demo and Power Plant in a nuclear environment. While NSST is an inherently pulsed device, CTF operates steady-state. The schematics in Fig. 2 illustrate the engineering and technology design contrasts for NSST and CTF. Because of the nuclear and engineering constraints, the CTF facility will quite limited in terms of physics tools and diagnostic capabilities compared to NSST.

2. Mission and Basic Device Design Parameters of NSST

2.1. Next-Step Performance Extension ST - NSST is envisioned as a "performance extension" (PE) stage ST with Ip x A ≈ 8 – 16 MA, which is similar in Ip x A to PE tokamaks such as JET, JT-60, and TFTR. It should be noted that the quantity Ip x A has been used as an approximate indicator of a tokamak device performance n x τ x T [6]. The Ip dependence signifies the importance of plasma current in device performance and the aspect ratio "A" reflects the unfavorable effect of toroidicity on confinement. Interestingly, the orignal 1984 paper [5] basing on the so-called L-mode scaling predicted stronger toroidicity scaling of ~ Ip x $A^{1.2}$ whereas more modern ITER confinment scaling (e.g., ITER-89P) tends to predict somewhat weaker toroidicity dependence of ~ Ip x $A^{0.8}$. Obviously having extensive confinement data base at low A from ST experiments would be a plus for the overall toroidal fusion physics understanding.

2.2 NSST Mission - The primary mission elements of NSST are to conduct spherical torus research at fusion plasma parameters to

1) Provide sufficient physics basis for the design of a compact CTF,
2) Explore advanced physics and operating scenarios with high bootstrap current fraction / high performance sustained advanced ST regimes, which can then be utilized on CTF, DEMO, and/or Power Plants, and
3) Contribute to the general plasma / fusion science of high □ toroidal plasmas including astrophysics.

2.3. Recent Progress on the ST Database - For NSST and future ST facilities, it is crucial to have an adequate experimental database as well as theory and modeling to be able to predict the plasma performance. Indeed, the progress in the ST plasma research being conducted worldwide has been quite rapid and encouraging [7, 8]. In the area of high beta operations, the high average toroidal beta values of $<\beta_T> \sim 35\%$ were achieved at high plasma current of Ip ~ 1.2 MA with $E_T \sim 200$ kJ of stored energy on NSTX [9], which is a significant progress from the previous START high beta results obtained with Ip ~ 0.2 MA with $E_T \sim 20$ kJ [10]. In another experiment, the high normalized beta value of $\beta_N \approx 6.5$ ($\beta_N \approx$ 10 li) was achieved where the so-called no-wall beta limit was significantly exceeded by about 35% [11]. In the area of plasma confinement, the observed global plasma energy confinement time in the NBI heated NSTX and MAST plasmas exceed the conventional confinement scalings both in H-mode and L-mode, diverted as well as inboard-limited plasmas [8, 12]. In Fig. 3, the global H-mode confinement data obtained in NSTX during the quasi-stationary phase of a discharge is shown. The red points are the experimental confinement time computed from the global stored energy from EFIT reconstruction and the input hearing power. The green points show a more recent assessment of the thermal plasma confinement time where the energetic component and the prompt beam loss components have been estimated by the TRANSP modeling code [12]. The NSST base performance projection assumes HH = 1.3 - 1.4 to obtain Q = 2 performance. The NSST Q performance is strongly dependent on the HH value so it is clear that the confinement and transport area is a high leverage research area for STs. In the area of integration, high poloidal-beta H-mode discharges ($\varepsilon\beta_p \sim 1$) at 800 kA were obtained with a significant non-inductive current fraction of ~ 60 % in NSTX as shown in Fig. 4 These discharges had good overall plasma performance parameters of $<\beta_T> \approx 16\%$, $\beta_N \approx 6$, HH ≈ 1.3, $H_{89P} \approx 2.5$ or β_N x H_{89P} of 15. Moreover, due to the low loop voltage (~ 0.1 V compared to 0.5 V for typical NBI heated discharges), the high poloidal beta regime was maintained for over τ-skin or about 5 τ_E [9]. It is noted that these dimensionless plasma parameters achieved in NSTX (except for the pulse length) are already approaching those needed for a CTF. Since the 2000 IAEA meeting, the H-mode database for STs has been expanding rapidly. The H-mode operation is now routine on NSTX and MAST. The observed H-mode power threshold has been coming down and it is now well below 1 MW giving a reasonable confidence level to access H-mode in future devices such as NSST [13,14]. It should be also noted that the H-mode access has facilitated the attainment of high beta regimes in NSTX by providing broader pressure and current profiles [11], which are favorable for MHD stability. These high performance ST plasma parameters, already obtained at Ip ~ 1 MA, suggest promising operating regimes for NSST and, if they can be extended to the 5 -10 MA range on NSST, bode well for the ST fusion energy development path based on a compact ST CTF facility and an eventual ST Demo.

2.4 Base Physics Design Parameters of NSST - To guide in the selection of a design point which can meet the requirements of the NSST mission, a systems code was developed and a parametric study was performed [15]. Many promising design points have emerged. The Tokamak Simulation (TSC) Code was also used to validate the systems code findings. In Fig. 5, the targeted NSST parameter space is shown. The current sustainment regime at B_T = 1.7 T (τ-pulse = 20 sec ~ 3 τ-skin) is ideal for investigating the CTF-like regimes at moderate Q. Here, a half-swing of the ohmic heating (OH) coil (from initial pre-charge current ramped down to zero) can start up the plasma. Another important research aim of NSST is to demonstrate multi-MA non-inductive start-up. A demonstration of multi-MA start-up is essential to establish a design base for a toroidal CTF without an ohmic heating solenoid. To allow sufficient pulse time to investigate such non-inductive scenarios, NSST can operate for 50 sec at 6 MA with B_T = 1.1 T. Finally, to explore wider ST plasma parameter space, the NSST device can operate in a purely inductive mode up to 10 MA with B_T = 2.7 T with a 5 sec flat top using the full OH swing, where Q = 2 performance can be expected with HH = 1.4. This operating mode will enable an exploration of α-particle related physics in high β plasmas for τ-pulse ~ 5 τ_E. A TSC simulation for the 10 MA inductive case has yielded higher Q ~ 2 for HH = 1.3 due to the plasma profile effect. In Table 2, the key parameters are listed for the full inductive and non-inductive sustained cases shown in Fig. 4. As shown in the table, the NSST base parameters require relatively modest plasma beta and Greenwald density parameters.

3. NSST Device Design

3.1 NSST Device Design Overview - To achieve the NSST mission, a flexible NSST device design was developed [16]. An isometric view of NSST device and a device cross sectional view are shown in Figs. 6 and 7. The magnets are liquid nitrogen cooled to allow long pulse as well as high performance operation. To facilitate timely progress for the NSST research program, an innovative ohmic solenoid is designed into the baseline center stack design to deliver sufficient flux for 10 MA operation with full swing and 6 MA operation with half swing. As shown in Fig. 7, with the in-board PF-1 coils, a strong plasma shaping capability (elongation κ = 2.7, triangularity δ = 0.6) is incorporated in the design. In Fig. 8(a), a tokamak simulation code (TSC) simulation of an inductively driven 10 MA plasma cross-section is shown, confirming the strong plasma shaping capability with κ = 2.7, δ = 0.6. In Fig. 8(b), the no-wall MHD stability limit is shown as a function of κ for several values of δ for the plasmas with ~ 50% bootstrap current fraction. As shown in the figure, the beta limit of β_T ~ 30 % can be reached without the benefit of the stabilizing plates for κ = 2.7, δ = 0.6. It should be noted that the expected range of the NSST base β_T values are indicated in the figure, which are well below the β_T ~ 30 % beta limit. For example, the Q=2 high performance regime can be achieved with the plasma beta of only about 13% (see Table 2). This shows that Q can be raised further (if for example the confinement improves above HH = 1.4) without exceeding the beta limit. The increased plasma beta is also desirable for increasing the bootstrap current fraction, which is an important element of the plasma sustainment in advanced ST scenarios. If the wall stabilization can be utilized, the β_T value can be increased further toward 45% which is important for the advanced ST operations with high bootstrap fraction, relevant for DEMO and Power Plants. To explore the advanced ST regimes, NSST is designed with tightly fitted stabilizing plates to access the simultaneously high β_T and β_N (high bootstrap current fraction) regimes as shown in Fig. 7. The outboard PF coils are placed sufficiently far from the plasma to reduce local shape distortions. The device is designed with a removable center stack to facilitate remote maintenance and allow for the possibility of future upgrades. The present NSST design utilizes the TFTR-like site with the peak electrical power of 800 MW and energy per pulse of 4.5 GJ and long pulse auxiliary heating and current drive systems (30 MW of NBI and 10 MW of RF). To explore alpha-physics in high beta plasmas for the first time, the existing tritium handling capability will be utilized.

3.2 Toroidal Field (TF) Coils – The NSST TF Coil consists of 96 standard turns with removable joints. An overview schematic of the TF coil is shown in Fig. 9. The TF joint details are shown in Fig, 10. Like NSTX, NSST features a demountable TF coil design, which permits the “center stack” of the device (i.e. a component assembly which contains the TF Inner Legs, OH Coil Sections, PF1a coils, the inner section of the vacuum vessel, and PFCs) to be removed separately as an integrated assembly, which is shown in Fig. 11 (a). The TF inner legs consisting of 96 standard OFHC copper (Cu) turns, of wedged shaped conductors, arranged in two layers, are cooled by liquid nitrogen (LN_2) via passages extruded in the conductors. Each of the 96 TF conductors has an independent cooling path. The liquid nitrogen enters from one end of the inner TF conductor and enters into a corresponding outer

TF conductor at the other end through a connecting hose and then returns back to the original location through an outer TF conductor. Turn-to-turn transitions in the two layers proceed in opposite directions so as to cancel the net toroidal current. The assembly is fabricated in a fashion similar to NSTX, except a high temperature, high shear stress cyanate ester resin insulator is used since the inner TF coil is designed near the stress limit against the torsional shear stress due to the ohmic solenoid. Torsional loads arising from the OH radial field crossing the TF current are reacted through the outer TF coil legs. The TF joint design require some innovation to satisfy the stringent mechanical and electrical requirements while facilitating simplified joint disassembly for TF center-stack removal. One possible type of joint design is shown in Fig. 10. The radial flags are wedged into a hub assembly to form a monolithic structure. The connectors are slightly flexible in the radial direction to avoid the development of a large radial force on the flags, and to allow the outer legs to rest against their support structure. Torsional loads arising from the OH radial field crossing the TF current are reacted through the outer TF coil legs. Radial flags and connectors are used to make the joints between the inner legs and the outer legs as shown in Fig. 10.

The current density in the outer legs is relatively low and the temperature rise is less than 10ºC per pulse. They are cooled by the exit flow of nitrogen (gas initially; liquid at full cool-down) routed though extruded passages in the outer leg conductor. As shown in Figs. 7 and 9 the shape of the outer legs is chosen such that the outward magnetic pressure due to the TF current crossing with the TF field results in a constant tension in the support strap, with minimal vertical tension imposed on the inner legs. Compression rings are used to adjust the constant tension shape to suit the desired height of the TF coil assembly. With the constant tension, moment-free shape, the outer legs and associated support structure can be made relatively flexible in the axial direction, thereby allowing the thermal expansion and contraction of the inner leg assembly without generating large stresses. The outer leg out-of-plane forces due to the radial component of TF current crossing with the vertical field of the PF coils are transmitted to the strap assembly via the compression panels and straps. The intrinsic torsional rigidity of the strap/compression ring structure is supplemented by mechanical keys which transmit torsional loads to the "cage" surrounding the machine, which is formed by PF coil support columns and the compression rings as shown in Fig. 7. Shear panels between the PF support columns will be added if further analyses indicates the need for additional torsional stiffness.

3.3 Ohmic Heating Solenoid and Poloidal Field Coils - In Fig. 11(a), the ohmic solenoid as a part of the center-stack assembly is shown. A two-part OH coil design is used, consisting of two concentric sections, with different current density in each section to increase the total available flux. The sections are connected in series and carry the same current per turn. The outer section is much less stressed compared to the inner one. Since the outer coil has a much longer path, it uses standard oxygen-free copper (Cu) conductor, which is operated to its thermal limit. The inner radius of the outer section which is the highest field point is chosen such that the hoop stress is at the allowable limit for copper. The outer OH coil section is therefore both thermal and stress limited, simultaneously. The inner section, operating at a much higher field level compared to the outer one, requires special strength copper. Because of its exceptionally high strength and relatively high conductivity a beryllium copper (BeCu) alloy is used, and the inner layer reaches its thermal limit before it reaches its allowable stress. While one could further optimize the strength and conductivity of the alloy used for the inner OH coil to make it simultaneously stress and thermal limited, the decision to use BeCu is largely based on its extensive availablility and well known material properties. The OH coil sections are cooled by LN_2 flowing through the annular regions between the OH and TF coils and between the OH sections. The long path length of the OH coil winding makes it impractical to cool the coil by nitrogen cooling path through the conductor as in the case of TF. The bipolar swing of OH current is asymmetric about zero to exploit the higher strength of the conductors at cold temperatures during the first swing, with the ratio of the first swing of current to the second swing equal to 1.8. The end of the OH solenoid can be contoured as shown in Fig. 11 (b) to tailor the flaring out of the OH fringing field to reduce the local j x B torsional force on the inner TF bundle by a factor of two. This feature does add to the complexity of the OH solenoid. However it remains an option which can be used if needed in the final design.

The PF Coil System consists of 6 coil pairs symmetric about the device midplane. Current per turn is 24kA in all circuits, based on the rating of TFTR-like power supplies. The PF coils design is relatively conventional due to its simple geometry and modest performance requirements.

3.4 Vacuum Vessel and PFCs - A double walled vacuum vessel with integral shielding is used on NSST. The vessel is fabricated of 316SS. The inner wall is 19 mm thick and the (less stressed) outer wall is 16 mm thick. Welded ribs are provided between the inner and outer walls to stiffen the structure. The inner space between walls is filled with 60% 316SS balls and 40% water to provide adequate shielding of device externals to the expected neutrons during the D-T operation. Ports are based on 16-fold symmetry. Four (4) midplane ports are assigned to the tangential access for the NBI injectors. Eight pairs of 6" diameter ports are included to accept feed-throughs for an 8 strap RF antenna subtending $8x7.5^o = 60^o$. The remaining nine rectangular midplane ports are 61 cm wide x 91 cm tall. Sixteen 30.5 cm diameter ports are provided on upper and lower domes, total 32. An ample plasma access is provided for plasma profile diagnostics to facilitate NSST research. The inner wall of the vacuum vessel (i.e., the center-stack casing) is formed by the 5 mm thick Inconel "center stack casing". Bellows assemblies and flanges are provided to allow for differential thermal expansion with respect to the outer vacuum vessel. The power and particle handling is a challenging issue for NSST and it is anticipated that the PFCs will be actively cooled for heat removal. The same cooling path will be used to heat the tiles for high temperature bakeout. The initial PFC (Plasma Facing Component) material will be graphite tiles due to the extensive operational experience. However more advanced PFCs can be considered for the DT operations in which tritium retention may become an issue.

3.5. Remote Maintenance - The NSST's unique configuration permits a relatively simple remote maintenance system. The doubled walled vacuum vessel is an effective shield such that work restrictions around the machineshould be similar to those of the large DT tokamak experiments such as TFTR. So, we can utilize the extensive DT experience from those tokamak experiments including many of the procedures. Remote maintenance is however required for the the internal components after the initiation of the D-T campaign for NSST. The ST geometry provides a unique opportunity for relatively simple remote maintenance. It is envisioned that the remote maintenance will be performed with the center-stack removed from the device as illustrated in Fig. 13. The center stack is lowered into the basement as shown in Fig. 13 (a). After the removal of the center stack, the access to the vacuum vessel internals becomes rather straight forward since an opening of about 2 m diameter becomes available. Through this opening a simple robotic arm with less than 3 m reach on a movable (vertically and rotatable) platform placed at the machine center can reach the entire internal surfaces of NSST as shown in Fig. 13 (b). The remote maintenance of the removed center-stack can be also performed with a relatively simple set up as shown in Fig. 13 (c). With the center-stack placed on a rotatable pedestal, a relatively short maintenance robotic arm system placed on a vertically moveable platform allows remote maintenance of the entire centerstack surface. The removal of center-stack thus allows a cost effective maintenance and repair of the internal vacuum vessel component as well as the center stack. Since the cost of such remote maintenance systems (the platforms and remote arms) is relatively modest, they might be useful not only for the D-T campaign but also during the initial D-D phase of operations. An early introduction of such remote maintenance systems would increase the installation precision and reduce the personnel safety risks of working inside the relatively large vacuum vessel as well as on the relatively tall center stack.

4. Physics Capabilities and Opportunities

4.1 Heating and Current Drive - The baseline heating and current drive system for NSST is the 110 keV - 30 MW NBI system and 10 MW of Ion Cyclotron Range of Frequency (ICRF) and High Harmonic Fast Wave (HHFW) system. The choice of NBI and ICRF is based on the relatively extensive experience and theoretical understanding of both heating and CD systems in Tesla-range experiments. The existing 30 MW NBI and 10 MW ICRF facilities are well developed and can be implemented at low cost and with low risk. The NBI beam ion confinement is expected to be excellent in NSST even accounting for possible losses due to MHD activities such as TAEs and Fishbones. The 30 MW NBI is expected to provide reliable baseline heating and current drive. The NBI also provides other important functions such as toroidal rotation and core fueling. It should be noted that NBI could also provide a platform for advanced plasma diagnostics.

The physics issues related to the ICRF (Ion Cyclotron Range of Frequency) /HHFW (High Harmonica Fast Wave) system are more challenging due to the three different operating magnetic field regimes. For the high performance DT burning regime operating at $B_T = 2.6$ T, the main objectives of ICRF is to heat the plasma core as needed. For this case, the well developed He_3-D or $2\Omega_T$ appears to be most suitable with $f \approx 20 - 25$ MHz range. For lower field, long pulse non-inductive operations, ICRF will be used as plasma start-up and current drive tools. Since this regime is expected to operate mainly with deuterium, second or third harmonic deuterium heating can be expected. In this regime while the electron Landau and magnetic pumping absorption processes can be strong due to relatively high beta value of the plasmas, one must also estimate the power absorbed by deuterium cyclotron harmonic damping. One could also consider going toward higher frequency of high harmonic fast wave to avoid ion absorption.

4.2 The NBI Induced Plasma Rotation - One of the long term goals of NSST research is to access the advanced ST regime. If successfully demonstrated, it could impact the operational scenarios of the CTF by supporting higher performance operations. In addition, it would support the design of Demo and power plants operating at higher beta. To foster advanced ST research, we have chosen tangential Neutral Beam Injection (NBI) as a reliable means to impart toroidal momentum to the plasma together with tightly fitted stabilizing plates. In Fig. 12, the NBI top view geometry is shown. In Fig. 13(a), the injected radial toroidal toque profile as calculated by TRANSP is shown where four co-injected beam lines are used. The resulting toroidal rotation velocity is shown as a function of the major radius. Here the toroidal angular momentum diffusivity is assumed to equal the neoclassical ion thermal diffusivity. In NSTX, the toroidal angular momentum of about 1/3 of the neoclassical values has been observed [12]. Therefore the neoclassical-like angular diffusivity assumption used for NSST is relatively conservative. As shown in the figure, the toroidal rotational speed could reach 600 km/sec or 35% of the local Alfven velocity in NSST. Since the rotational speed needed for the RWM stabilization is typically a few percent of the Alfven velocity, the generation of sufficient toroidal rotation should be readily achievable in NSST. We can therefore consider placing one of the four NB injectors in the counter-direction to introduce additional physics flexibility. The remaining three NB injectors will be installed in the co-direction at various injection angels and tangency radii. This will potentially allow finer control of the rotational velocity per given injected NBI power as well as control of the heating and current drive profiles and velocity sheared layer locations for the ITB formation to control for example the pressure profile.

4.3 Non-Inductive Start-Up - Non-inductive start-up research is a central topic for NSST, particularly, to demonstrate multi-MW level non-ohmically driven start-up current. At present, NSTX is investigating coaxial helicity injection (CHI) plasma current start-up, which has succeeded in driving about 400 kA of toroidal current with injection of 27 kA at about 700 V bias voltage [6, 17]. Recently, on the HIT-II device, an experiment was conducted to show significant ohmic volt-second savings by the initial application of CHI [17]. While CHI is still under development, the trend from HIT-II to NSTX seems to show a favorable scaling of a factor of two improvement in the current multiplication (i.e., the ratio of the generated toroidal current to the injected CHI current.) The expected CHI requirement increases with the desired plasma start up current and the plasma size but decreases with the plasma temperature due to slower current dissipation. Using similar scaling from HIT-II to NSTX, the current multiplication can be expected to be about three times larger on NSST compared to NSTX for the same injector flux and voltage. In addition, by going to higher voltage (2 – 3 kV), which is likely to be needed to operate at much higher toroidal field in NSST compared to NSTX, it appears to be feasible to drive 5 MA of toroidal current with injection current of only about 30 kA. It is therefore important to understand this scaling through experiments as well as 3-D numerical simulations before finalizing the CHI design for NSST. The removable feature of the NSST centerstack should permit the incorporation of the required CHI insulator if the CHI technique can be shown to be extendable to multi-MA level plasma current.

With its long pulse length of 50 sec, NSST can also test other innovative non-inductive current drive techniques, such as bootstrap over-drive using rf based heating as invoked in the ARIES-ST /AT study. The recent JT-60U experiment on non-ohmic plasma start-up using modest ohmic induction, rf and NBI current ramp-up, NBI heating induced bootstrap over-drive, and vertical field ramp-up to obtain Ip = 600 - 700 kA is very encouraging [18]. The NSST could further develop this technique toward multi-MA regimes needed for the design and construction of a CTF facility. On NSST, we can utilize a modest amount of ECH or EBW (electron Bernstein waves) power [19] to initiate the plasma discharges and the 10 MW ICRF system in a HHFW (High harmonic fast wave) heating and current drive mode [20] to ramped up the plasma current. After the plasma current reaches an adequate level for the NBI confinement (> 1MA), the 30 MW NBI heating can be turned on to heat and densify the plasma to high-poloidal-beta / high bootstrap current fraction to reach multi-MA current. The optimization of the poloidal/vertical fields as done for the JT-60U is also a very important part of the study. The demonstration of nonohmic start-up technique is considered to be essential for an ST-based compact CTF as well as power plants.

4.4 α -Particle Physics - In Table 3, some relevant physics dimensionless parameters are listed for representative ST devices. In terms of the α-particle related physics, a key dimensionless parameter is V_α/V_{Alf} which is about 4 - 5 for NSST but also the similar values for the future devices such as CTF and ARIES-ST reactor. This value is also comparable to the values attained on NSTX with NBI where $V_{NBI}/V_{Alf} \approx 3$. On NSTX, NBI heated discharges indeed yielded a variety of high frequency MHD modes including TAEs (Toroidal Alfven Eignmodes) at 100 kHz range and CAEs (Compressional Alfven Eigenmodes) at few MHz range (starting from near the half deuterium cyclotron frequency). In NSTX, CAEs are not observed to cause any NBI ion particle losses but there is an interesting theoretical prediction of CAEs stochastically heating bulk ions [121]. This prediction was stimulated by the apparent observation of unusually high ion temperature discharges on NSTX during NBI [12]. If proven to be true, this direct ion heating by α-particles can further enhance the high Q operational regimes in ST reactors. The NSST device and its physics diagnostic capabilities should therefore yield important reactor relevant α-particle related physics data as well as the isotope scaling in high beta toroidal plasmas for the first time. In the 10 MA NSST discharges, the alpha particle orbits are estimated to be relatively well confined [22].

5. Summary and Future Plans

The spherical torus concept can contribute effectively to the fusion energy development path (i.e., NSTX/MAST, NSST, CTF, and DEMO). The ST development path is complementary to the tokamak-based burning plasma experiments as it focuses on a compact CTF facility and exploration of higher toroidal beta regimes for Demo and Power Plant reactors. The CTF facility can provide a test bed for the development of blanket modules and other fusion core components, exposing them to high neutron wall loading and accumulated fluence. As an ST Performance Extension level experiment, the NSST facility can provide the necessary physics basis for the design and construction of a compact ST-based CTF, while developing more advanced physics scenarios for CTF, DEMO and ST power plants. To support its mission, the NSST facility, with up to 10 MA of plasma current, is designed with ample advanced physics features such as strong plasma shaping and wall mode stabilizing plates as well as physics tools including the NBI system to drive sufficient toroidal rotation and rotational shear flows for improved stability and confinement, and with ample diagnostic access to facilitate physics research. Tritium operation will enable alpha-particle and isotope scaling research at high beta for the first time providing valuable data base for an attractive Demo design. The removable center-stack design can facilitate the remote maintenance of the NSST internal hardware.

ACKNOWLEDGEMENTS:

Work is supported by U.S. Department of Energy under contracts DE-AC05-00OR22725 and DE-AC02-76CH03073, and grants. Thanks are due to the NSTX Research Team for providing pertinent data for the NSST design, R. Goldston and R. Hawryluk for advice and encouragements, and S. Jardin for expert help in the analysis codes.

REFERENCES:

[1] M. Peng, J. B. Hicks, Fusion Technology 1990, **2**, 1287 (Elsevier Science Publishers B. V., 1991).

[2] M. Peng et al., Fusion Engineering, 1997, 17th IEEE/NPSS Symposium **2**, 733 (1998).

[3] I. V. Sviatoslavsky et al., Fusion Engineering and Design, **45**, 281(1999).

[4] M. A. Abdou et al., Fusion Technology, **29**, 1(1996).

[5] FESAC Panel of Development Path. A Plan for Development of Fusion Energy, Preliminary Report to FESAC, issued in March 2003.

[6] R.J. Goldston, Plasma Physics and Controlled Fusion, **25**, 874 (1984).

[7] E. Synakowski et al., "The National Spherical Torus Experiment (NSTX) Research Program and Progress Towards High Beta, Long Pulse Operating Scenarios," IAEA-CN-94/OV/2-2 Fusion Energy 2002 (Proc. 19^{th} Int. Conf. Lyon, 2002).

[8] B. Lloyd et al., "Overview of Recent Experimental Results on MAST," IAEA-CN-94/OV/2-3, Fusion Energy 2002 (Proc. 19^{th} Int. Conf. Lyon, 2002).

[9] J. Menard et al., "Beta-limiting MHD Instabilities in NSTX Spherical Torus Plasmas," IAEA-CN-94/ EX/S1-5, Fusion Energy 2002 (Proc. 19^{th} Int. Conf. Lyon, 2002).

[10] M. Gryaznevich et al., Phys. Rev. Letters <u>80</u>, 3972 (1998).

[11] S. Sabbagh et al., "The Resistive Wall Mode and Feedback Control Physics Design in NSTX," IAEA-CN-94/EX/S2-2, Fusion Energy 2002 (Proc. 19^{th} Int. Conf. Lyon, 2002).

[12] B. LeBlanc et al., "Confinement Studies of Auxiliary Heated NSTX Plasmas," IAEA-CN-94/ EX/C5-2, Fusion Energy 2002 (Proc. 19^{th} Int. Conf. Lyon, 2002).

[13] R. Maingi, et al., "H-mode Research in NSTX," IAEA-CN-94/ EX/C2-5, Fusion Energy 2002 (Proc. 19^{th} Int. Conf. Lyon, 2002).

[14] P.G. Carolan, et al., "H-mode Access Physics in MAST," IAEA-CN-94/ EX/C2-6, Fusion Energy 2002 (Proc. 19^{th} Int. Conf. Lyon, 2002).

[15] S.C. Jardin, C.E.Kessel, D. Meade,, and C.L. Neumeyer, Fusion Science and Technology **43**, 161 (2003).

[16] C. Neumeyer, et al., "Spherical Torus Center Stack Design", C Neumeyer et al, Proceedings of the 19th IEEE/NPSS Symposium on Fusion Engineering (SOFE), January 2002, Atlantic City, NJ, IEEE No. 0-7803-7073-2/02, pg. 413-417.

[17] T. Jarboe, et al, "Progress with Helicity Injection Current Drive," IAEA-CN-94/ IC/P-10 Fusion Energy 2002 (Proc. 19^{th} Int. Conf. Lyon, 2002).

[18] Y. Takase, et al., the Journal of Plasma and Fusion Research,**78**, 719-721 (2002).

[19] P. Efthimion et al, "Application of Electron Bernstein Wave Heating and Current Drive to High Beta Plasmas," IAEA-CN-94/ EXP/2-12, Fusion Energy 2002 (Proc. 19th Int. Conf. Lyon, 2002).

[20] P. Ryan et al, "RF Heating and Current Drive on NSTX with High Harmonic Fast Waves," IAEA-CN-94/ EXP/2-13, Fusion Energy 2002 (Proc. 19th Int. Conf. Lyon, 2002).

[21] N. Gorelenkov et al, "Theory and Observation of Compressional Alfven Eigenmodes in Low Aspect Ratio Plasma," IAEA-CN-94/ EX/W-7, Fusion Energy 2002 (Proc. 19th Int. Conf. Lyon, 2002).

[22] D. Darraw et al, "Measurements and Modeling of Prompt, Non-Adiabatic, and MHD-induced Fast Ion Loss from Spherical Tokamaks," IAEA-CN-94/ EXP/P2-01, Fusion Energy 2002 (Proc. 19th Int. Conf. Lyon, 2002).

Table 1. Key device and plasma parameters for three representative devices for the ST fusion energy development path.

	NSTX	NSST	CTF
R(m)	0.85	1.5	1 – 1.5
a(m)	0.65	~0.9	~ 0.7 - 1
□, □	2, 0.8	~2.7, ~0.6	~ 3, ~ 0.5
I_p (MA)	1.5	~ 5 - 10	~ 10 –12
B_T(T)	0.3 – 0.6	~1.1 – 2.6	~ 1.7 – 2.1
Pulse (s)	5 - 1	~ 50 - 5	Steady-state
TF	Multi-turn	Multi-turn	Single- turn

Table 2: Key plasma and device parameters for full inductive and non-inductive sustained regimes.

	Full Inductive	Non-Inductive Sustained
B_t (T)	2.6	1.15
$□_T$ (%)	13.3	26.3
$□_N$ (%)	3.2	4.64
$<n_e>$ ($10^{20}/m^3$)	2.1	1.0
f_{GW} (%)	63.3	50.7
$<T_e>$ (keV)	5.5	4.5
$□_{skin}$ (sec)	9.3	4.9
HH(98pby2)	1.4	1.4
$□_E$ (sec)	0.7	0.36
Q	2	0.25

Table 3: Key physics dimensionless parameters for representative ST devices.

	NSTX	NSST	CTF	ARIES-ST
□*	0.2	0.04	0.02	0.015
$a/□_i$	35	130	108	140
$<□_□>$	0.35	0.4	0.2 - 0.4	0.5
V_{NBI}/V_{Alfven}	3	0.7		
$V_□/V_{Alfven}$		4.4	5.8	5

FIGURE CAPTIONS:

Fig. 1. ST contribution to the fusion energy development path. The present experimental devices including NSTX/MAST provide physics data base for the design of NSST. The NSST operating at 5 – 10 MA at fusion parameters provides necessary physics basis for CTF and high beta physics data for Demo. The CTF facility is dedicated to develop high performance reliable core components for Demo.

Fig. 2. Representative ST Device Schematics. The NSTX device at 1.5 MA is a proof-of-principle step to demonstrate the attractiveness of the ST concept. The NSST at 5 – 10 MA is a performance-extension step to demonstrate the physics viability of ST at fusion parameters. The CTF or Component Test Facility is envision to be a singl-turn-TF steady-state ST device with compact size and modest tritium consumption (~ 100 MW).

Fig. 3. Global Confinement Trends in NSTX. The red points are H-mode point where the confinement time was computed using the EFIT global stored energy and the NBI injected power. The green points are some initial correction with TRANSP to include only the thermal components and NBI deposited power removing the prompt loss.

Fig. 4. The discharge evolution of high β_p *shot in NSTX. The high beta poloidal discharge is obtained with significant ~ 60% non-inductive current drive with the loop voltage remain very low ~ 0.1 V. The bootstrap current fraction gradually increases in time due to similar density rise. The high beta poloidal regime is maintained for over the resistive skin time. The discharge becomes diamagnetic after 400 msec*

Fig. 5 NSST Operating Design Points. Three main operating regimes are shown. The 50 sec non-inductively sustained regime is aiming to develop ohmic solenoid free start-up and current sustainement concepts at multi-MA range for the pulse length much greater than the plasma skin time which is directly relevant for the design of CTF. The non-inductively assisted regime operates at higher plasma performance of Q ~ 0.5 for 20 sec or 2-3 skin time. This operation may use half-swing induction to ramp-up the current followed by strong non-inductive current drive for sustainment. The full inductive region employs double-swing induction to reach high current and high performance region of Q ~ 2 for 5 sec or about 10 energy confinement time. This regime is a candidate for a tritium operation to study alpha-physics at high beta, relevant for Demo.

Fig. 6. Isometric View of NSST. The outer TF is depicted in red and the poloidal coils are depicted in blue. The brown central column is the inner TF legs. The green cylinder around the inner TF depicts the ohmic solenoid. The stainless steel vacuum vessel is double walled filled with neutron absorbing material, The double-walled vacuum vessel and the supporting structures are shown in gray.

Fig. 7. NSST Device Cross Section. The vacuum vessel contains neutron absorbing material as partial shield to minimize the external activation. The passive plates are for the resistive wall stabilization with rotation.

Fig. 8. NSST Plasma MHD Stability Limit: (a) TSC simulation of 10 MA inductively driven highly shaped plasma. (b) No-wall MHD stability dependence of triangularity for various elongations with the bootstrap current fraction of ~50%.

Fig. 9. NSST Toroidal Coil schematics. The TF consists of 96 standard turns with removable joints. The inner TF conductor is wrapped with cynate ester insulation shich has higher shear strength at elevated temperature and better radiation resistance compared to standard epoxies. The torsional loads from OH is reacted through torque collar and TF joint flags to the hub assembly and to the outer TF support. Constant tension outer legs with compression rings and flexible straps are envisioned.

Fig. 10. TF joints details: (a) TF Joint overview schematic. Two layer 96 joint design. (b) Flag-to-Connecter Joint Concept Using Recessed Flag Studs and Cut-outs for Fasteners (c) Alternate NSST Flag-to-Connecter Joint Concept Using Over-Center Clamps To Facilitate Remote Handling.

Fig. 11. Ohmic heating solenoid design. (a) Two-layered OH solenoid design is shown in green around the inner TF bundle (in brown). The outer OH layer is made out of oxygen-free copper and the inner OH layer is made out of beryllium copper. The OH coil sections are cooled by LN_2 flowing through the annular regions between the OH and TF coils and between the OH sections. (b) A properly contoured OH solenoid end design to control the flaring of the OH fringing field pattern can reduce the local j x B force stress on the inner TF bundle.

Fig.12. Tangential NBI Access View. Relatively slender TF outer legs enables the tangential NBI access. One of four NBI beam boxes is envisioned to be placed in the counter direction to provide momentum input flexibility. The beam angles will be chosen to optimize the physics flexibility.

Fig. 13. NSST Remote Handling Schematics: (a) NSST Center Stack being lowered into the basement for maintenance. (b) A set-up for internal vacuum vessel component maintenance. (c) A set-up for Center-Stack maintenance.

Fig. 14. TRANSP simulation of NBI induced toroidal rotation: (a) Toroidal torque provided by NBI beam. (b) Resulting plasma toroidal rotation profile. .

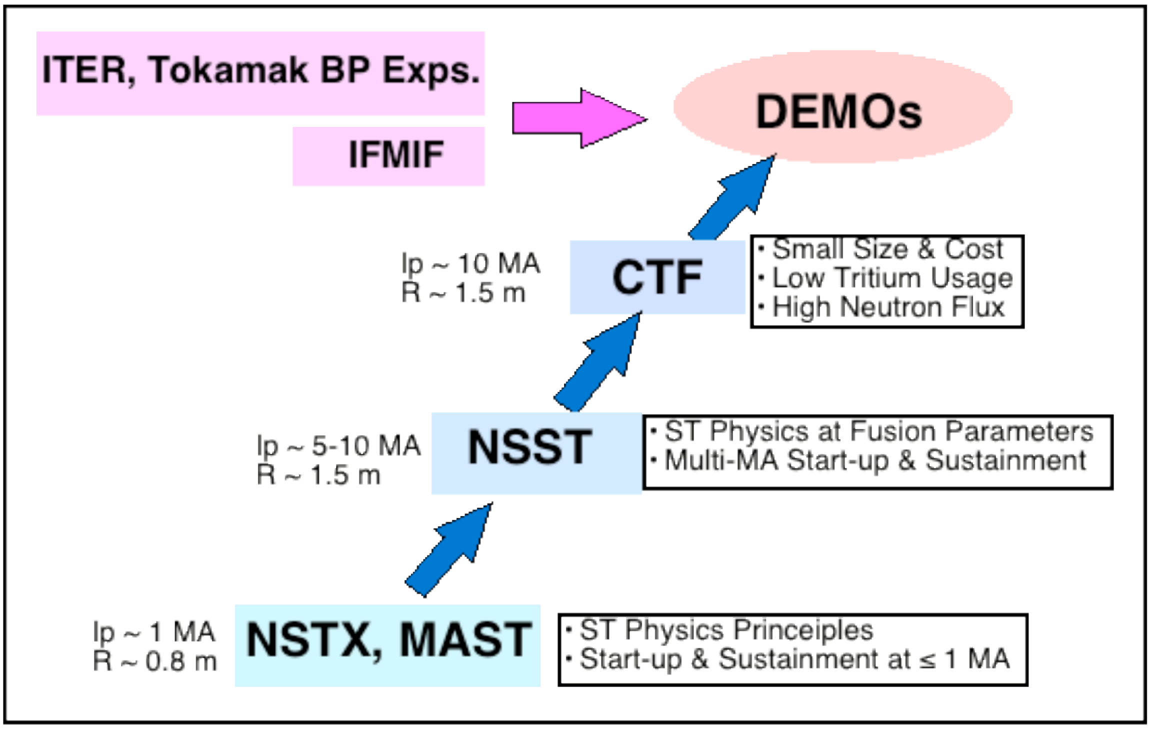

Fig. 1. ST contribution to the fusion energy development path. The present experimental devices including NSTX/MAST provide physics data base for the design of NSST. The NSST operating at 5 – 10 MA at fusion parameters provides necessary physics basis for CTF and high beta physics data for Demo. The CTF facility is dedicated to develop high performance reliable core components for Demo.

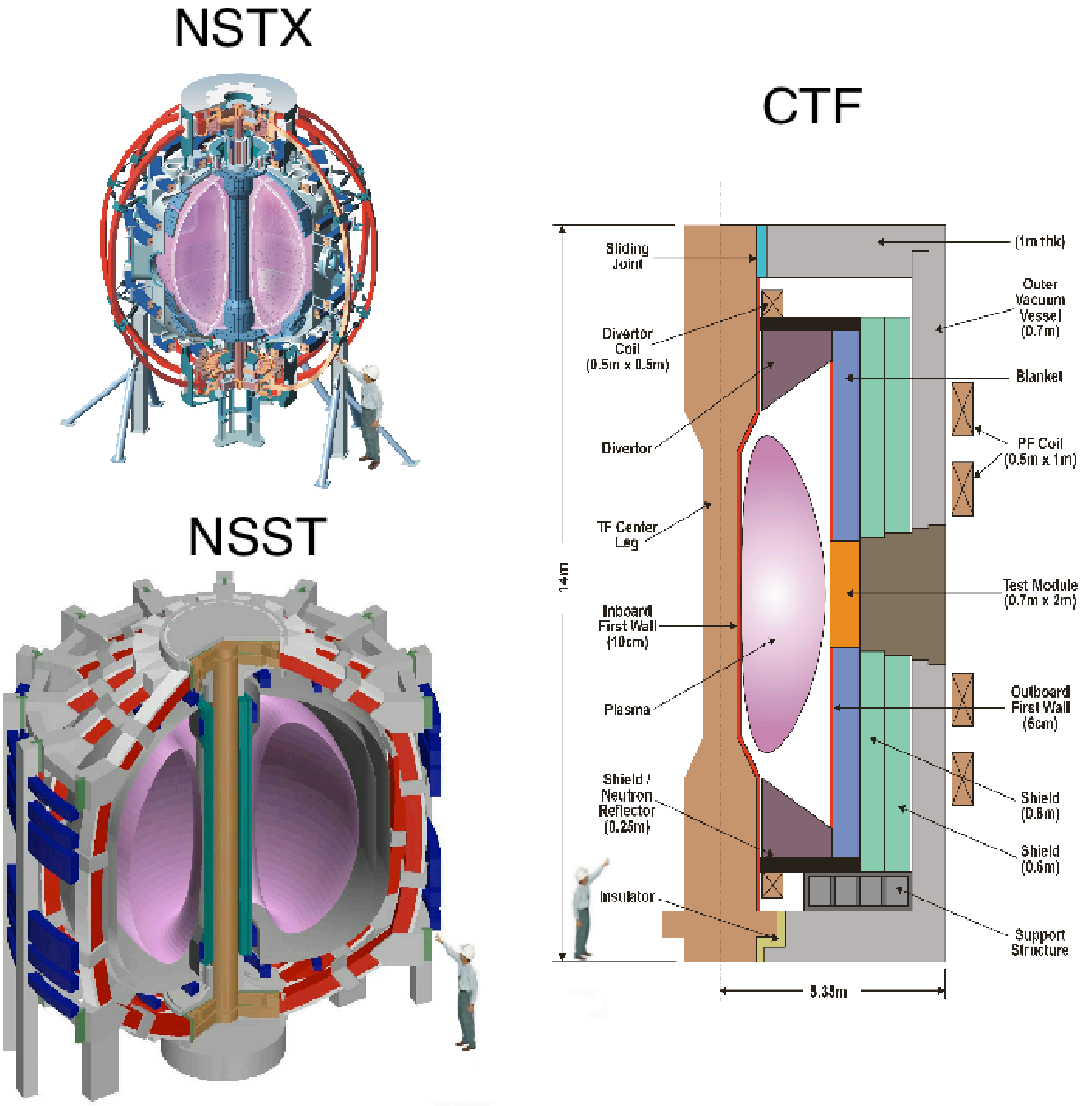

Fig. 2. Representative ST Device Schematics. The NSTX device at 1.5 MA is a proof-of-principle step to demonstrate the attractiveness of the ST concept. The NSST at 5 – 10 MA is a performance-extension step to demonstrate the physics viability of ST at fusion parameters. The CTF or Component Test Facility is envision to be a singl-turn-TF steady-state ST device with compact size and modest tritium consumption (~ 100 MW)

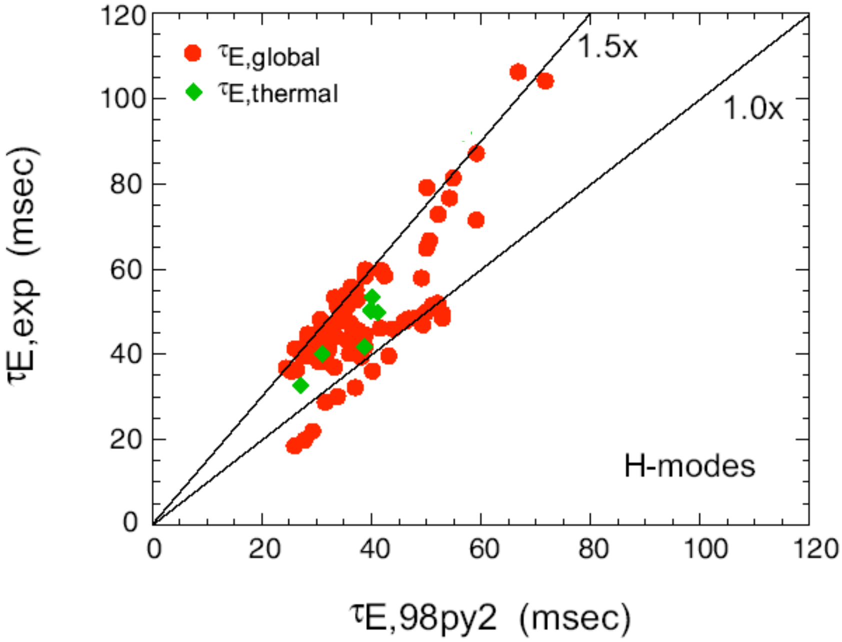

Fig. 3. Global Confinement Trends in NSTX. The red points are H-mode point where the confinement time was computed using the EFIT global stored energy and the NBI injected power. The green points are some initial correction with TRANSP to include only the thermal components and NBI deposited power removing the prompt loss.

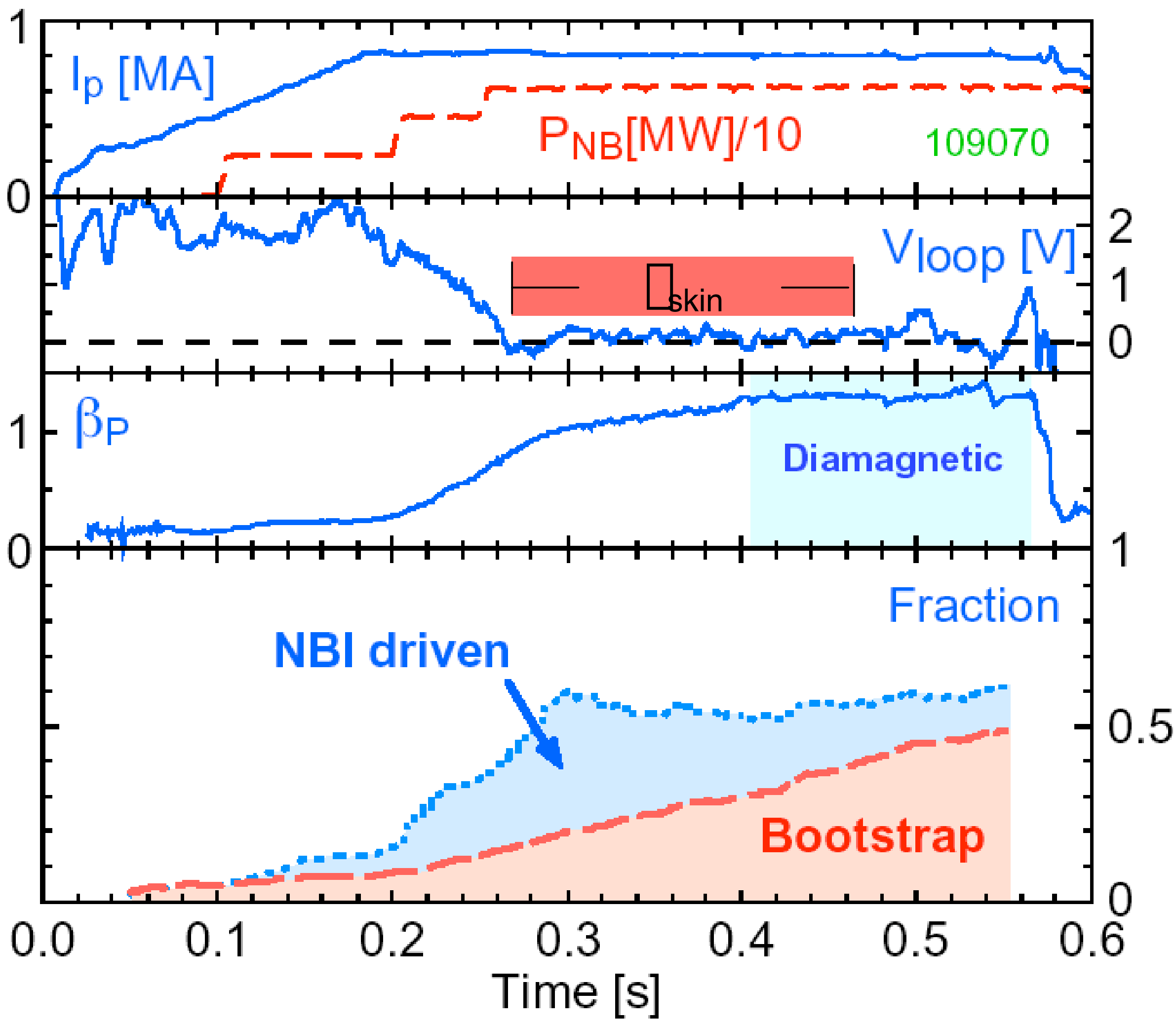

Fig. 4. The discharge evolution of high bp shot in NSTX. The high beta poloidal discharge is obtained with significant ~ 60% non-inductive current drive with the loop voltage remain very low ~ 0.1 V. The bootstrap current fraction gradually increases in time due to similar density rise. The high beta poloidal regime is maintained for over the resistive skin time. The discharge becomes diamagnetic after 400 msec

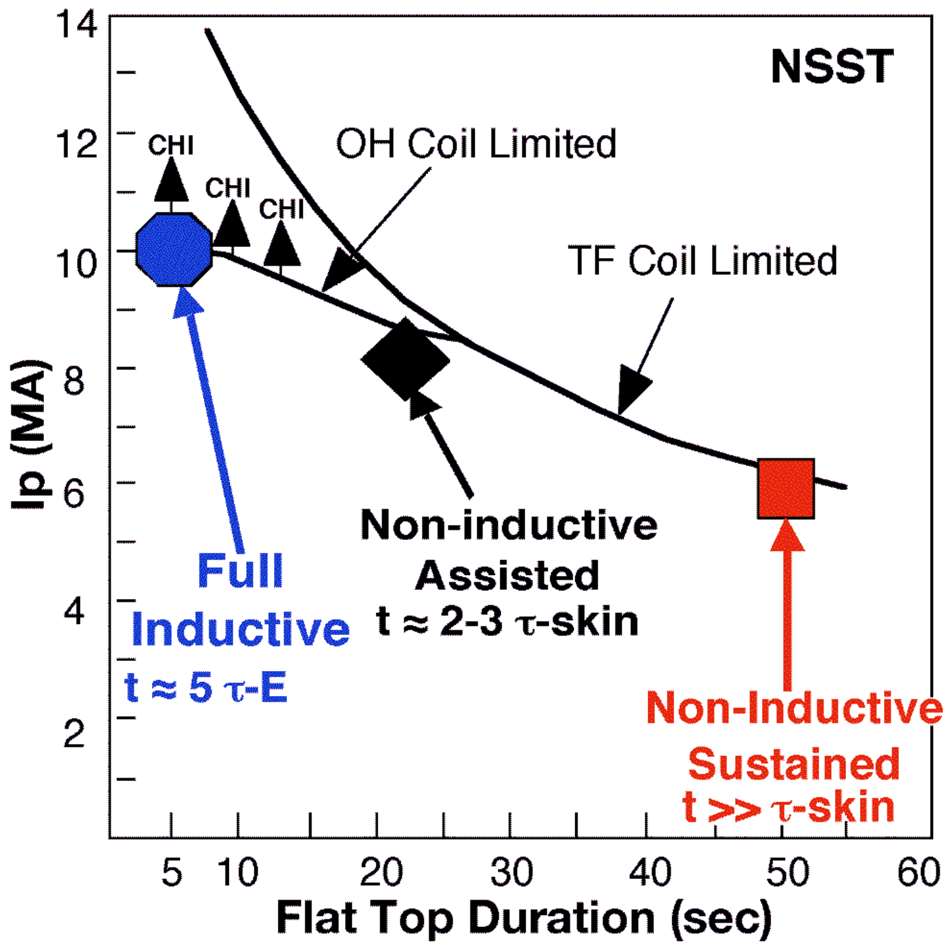

Fig. 5. NSST Operating Design Points. Three main operating regimes are shown. The 50 sec non-inductively sustained regime is aiming to develop ohmic solenoid free start-up and current sustainement concepts at multi-MA range for the pulse length much greater than the plasma skin time which is directly relevant for the design of CTF. The non-inductively assisted regime operates at higher plasma performance of Q ~ 0.5 for 20 sec or 2-3 skin time. This operation may use half-swing induction to ramp-up the current followed by strong non-inductive current drive for sustainment. The full inductive region employs double-swing induction to reach high current and high performance region of Q ~ 2 for 5 sec or about 10 energy confinement time. This regime is a candidate for a tritium operation to study alpha-physics at high beta, relevant for Demo.

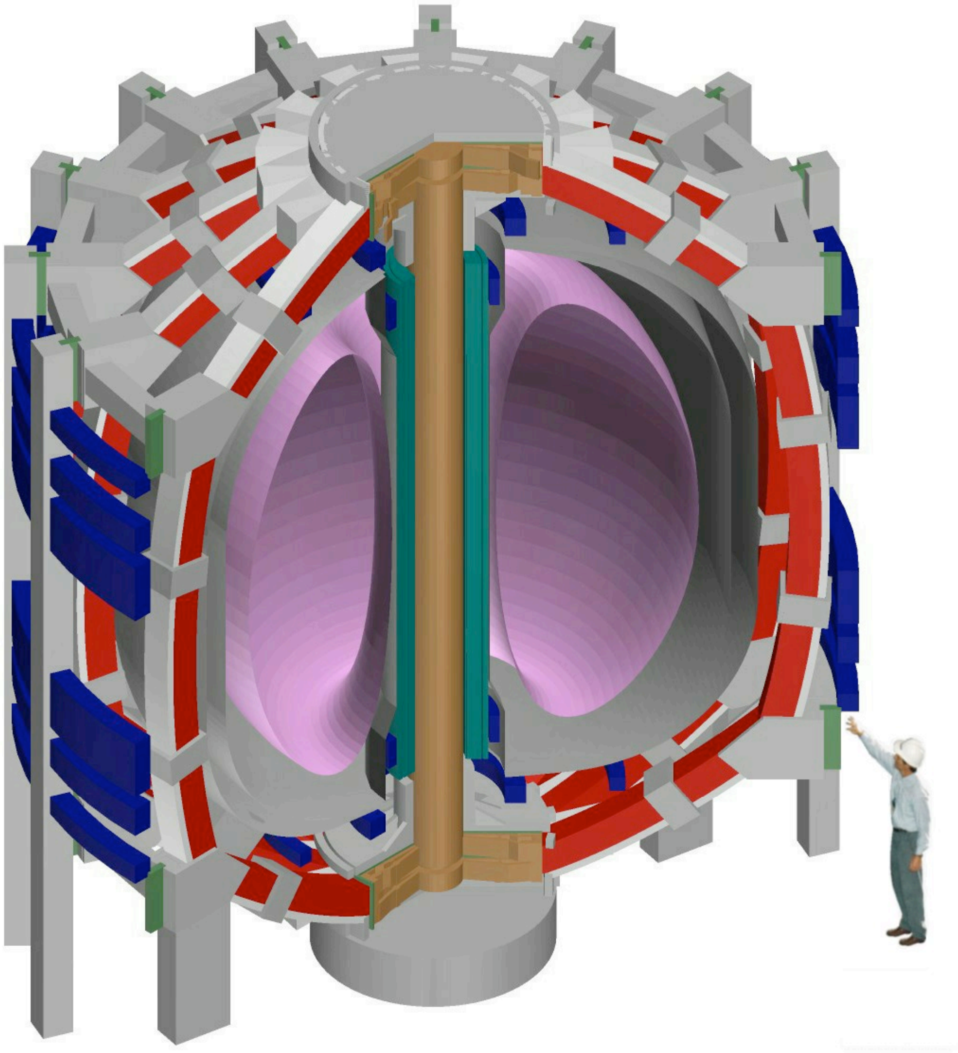

Fig. 6. Isometric View of NSST. The outer TF is depicted in red and the poloidal coils are depicted in blue. The brown central column is the inner TF legs. The green cylinder around the inner TF depicts the ohmic solenoid. The stainless steel vacuum vessel is double walled filled with neutron absorbing material, The double-walled vacuum vessel and the supporting structures are shown in gray.

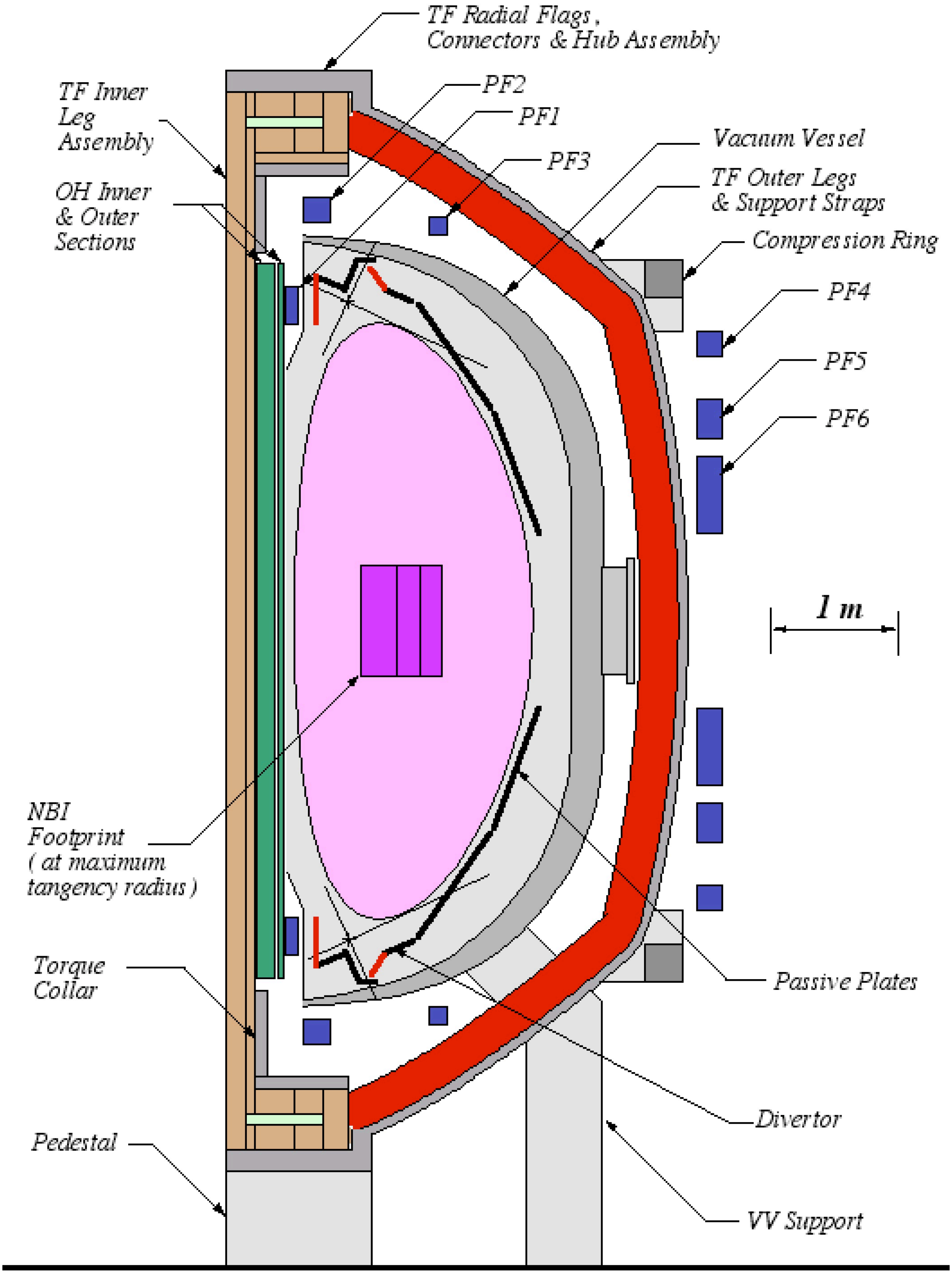

Fig. 7. NSST Device Cross Section. The vacuum vessel contains neutron absorbing material as partial shield to minimize the external activation. The passive plates are for the resistive wall stabilization with rotation.

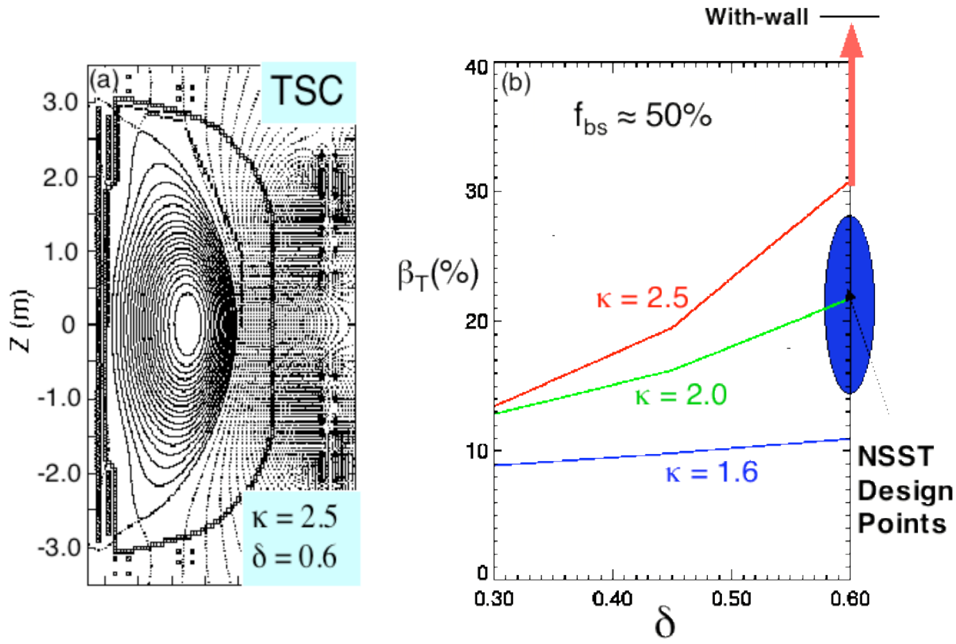

Fig. 8. NSST Plasma MHD Stability Limit: (a) TSC simulation of 10 MA inductively driven highly shaped plasma. (b) No-wall MHD stability dependence of triangularity for various elongations with the bootstrap current fraction of ~50%.

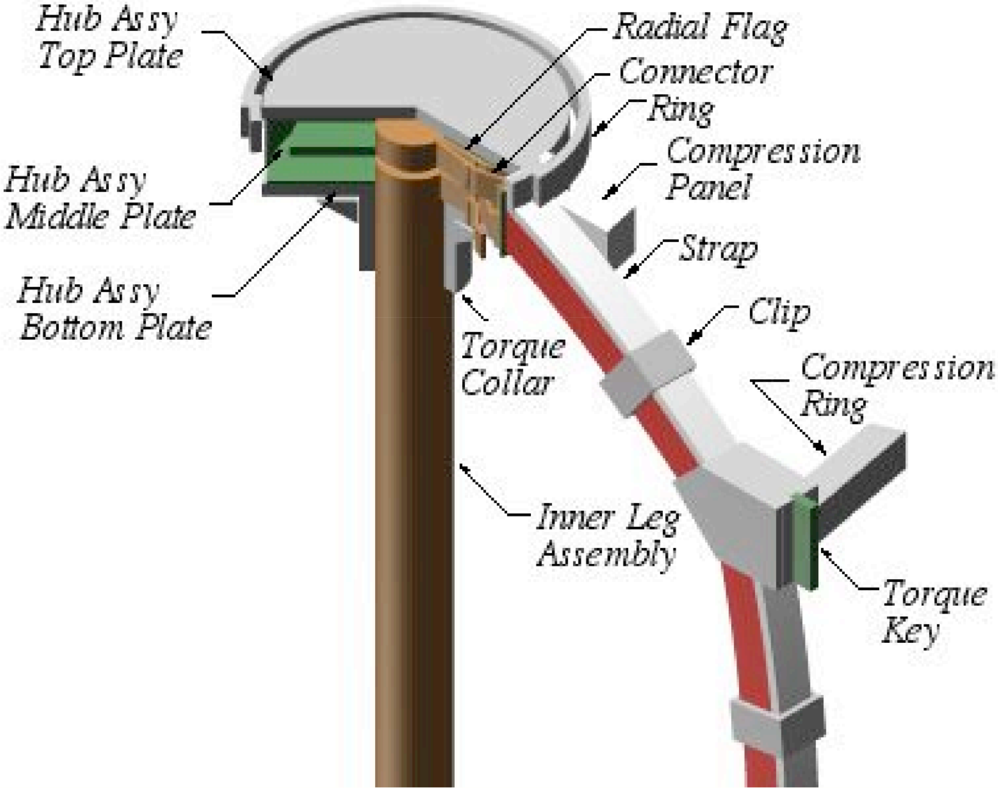

Fig. 9. NSST Toroidal Coil schematics. The TF consists of 96 standard turns with removable joints. The inner TF conductor is wrapped with cynate ester insulation shich has higher shear strength at elevated temperature and better radiation resistance compared to standard epoxies. The torsional loads from OH is reacted through torque collar and TF joint flags to the hub assembly and to the outer TF support. Constant tension outer legs with compression rings and flexible straps are envisioned.

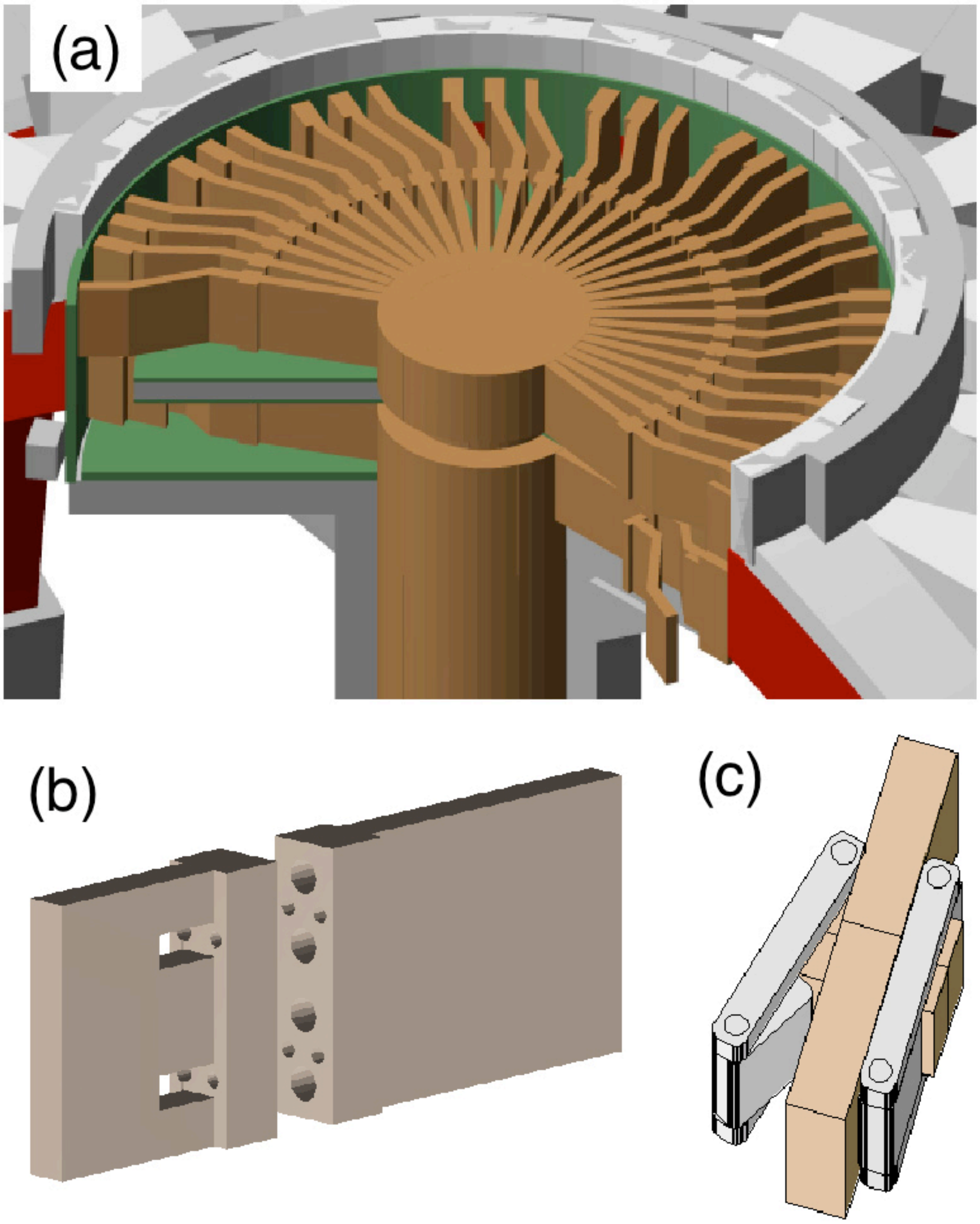

Fig. 10. TF joints details: (a) TF Joint overview schematic. Two layer 96 joint design. (b) Flag-to-Connecter Joint Concept Using Recessed Flag Studs and Cut-outs for Fasteners (c) Alternate NSST Flag-to-Connecter Joint Concept Using Over-Center Clamps To Facilitate Remote Handling.

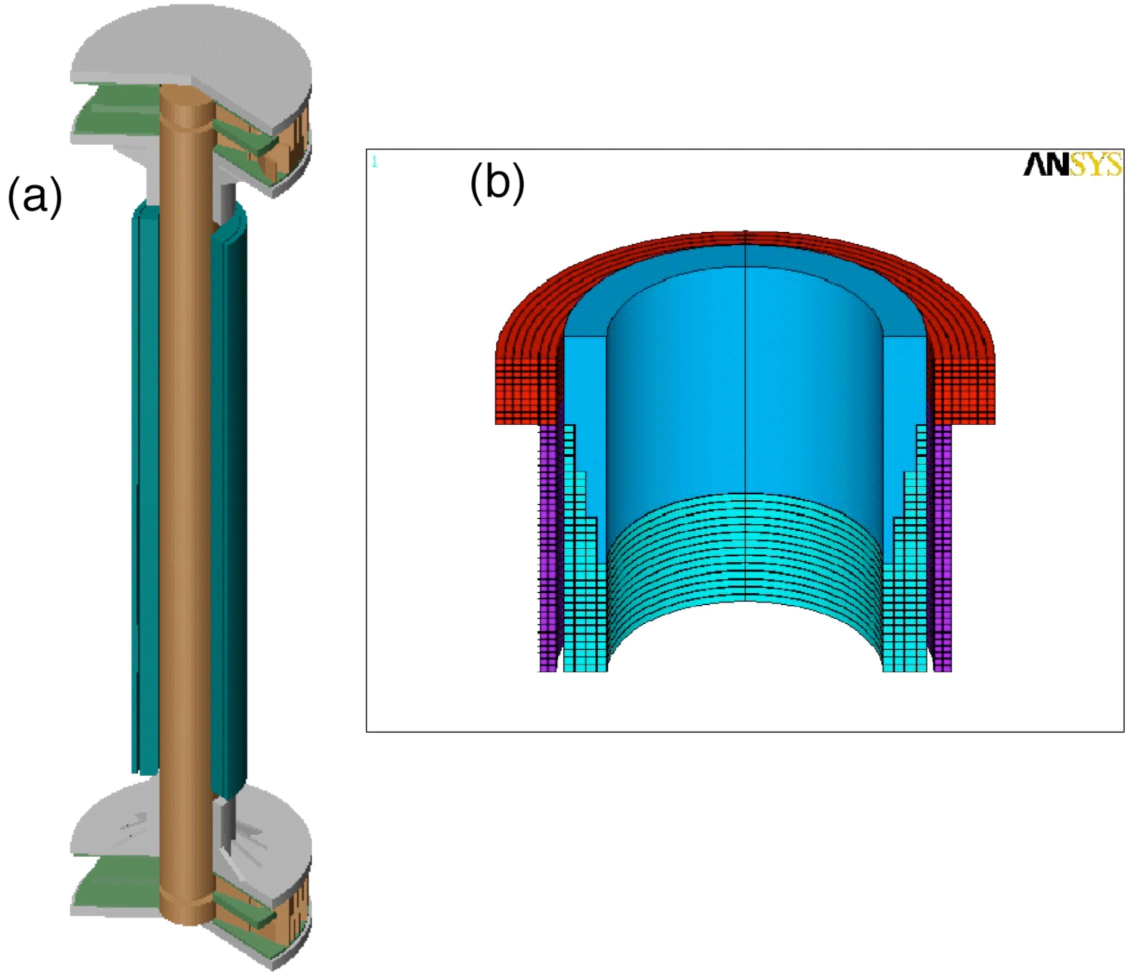

Fig. 11. Ohmic heating solenoid design. (a) Two-layered OH solenoid design is shown in green around the inner TF bundle (in brown). The outer OH layer is made out of oxygen-free copper and the inner OH layer is made out of beryllium copper. The OH coil sections are cooled by LN_2 flowing through the annular regions between the OH and TF coils and between the OH sections. (b) A properly contoured OH solenoid end design to control the flaring of the OH fringing field pattern can reduce the local j x B force stress on the inner TF bundle.

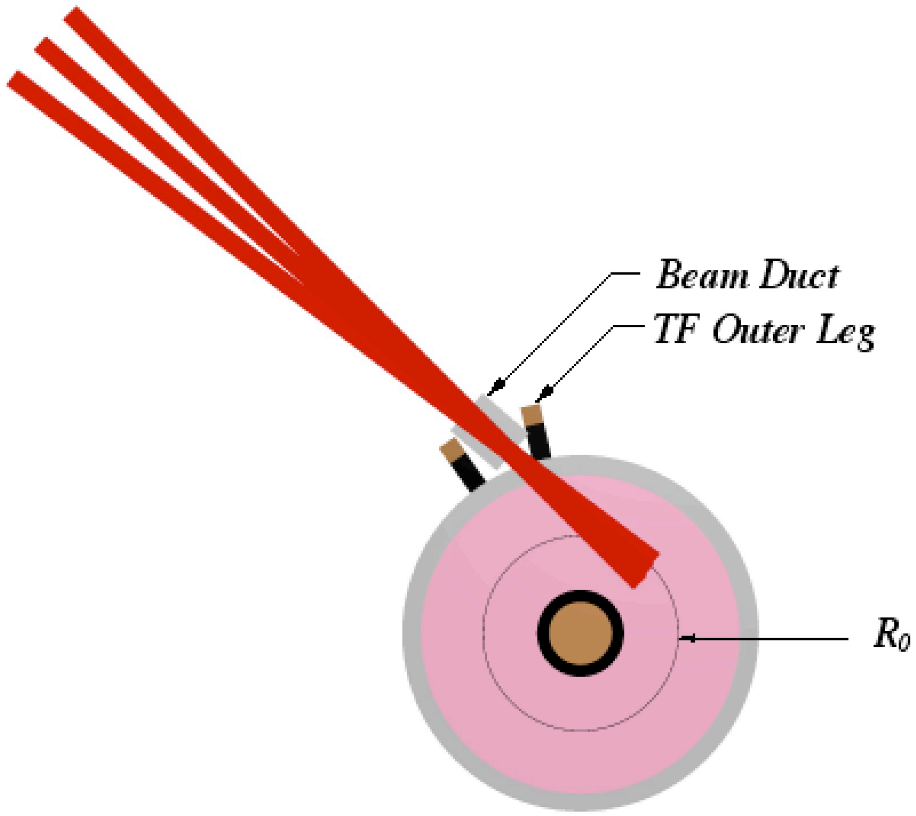

Fig. 12. Tangential NBI Access View. Relatively slender TF outer legs enables the tangential NBI access. One of four NBI beam boxes is envisioned to be placed in the counter direction to provide momentum input flexibility. The beam angles will be chosen to optimize the physics flexibility.

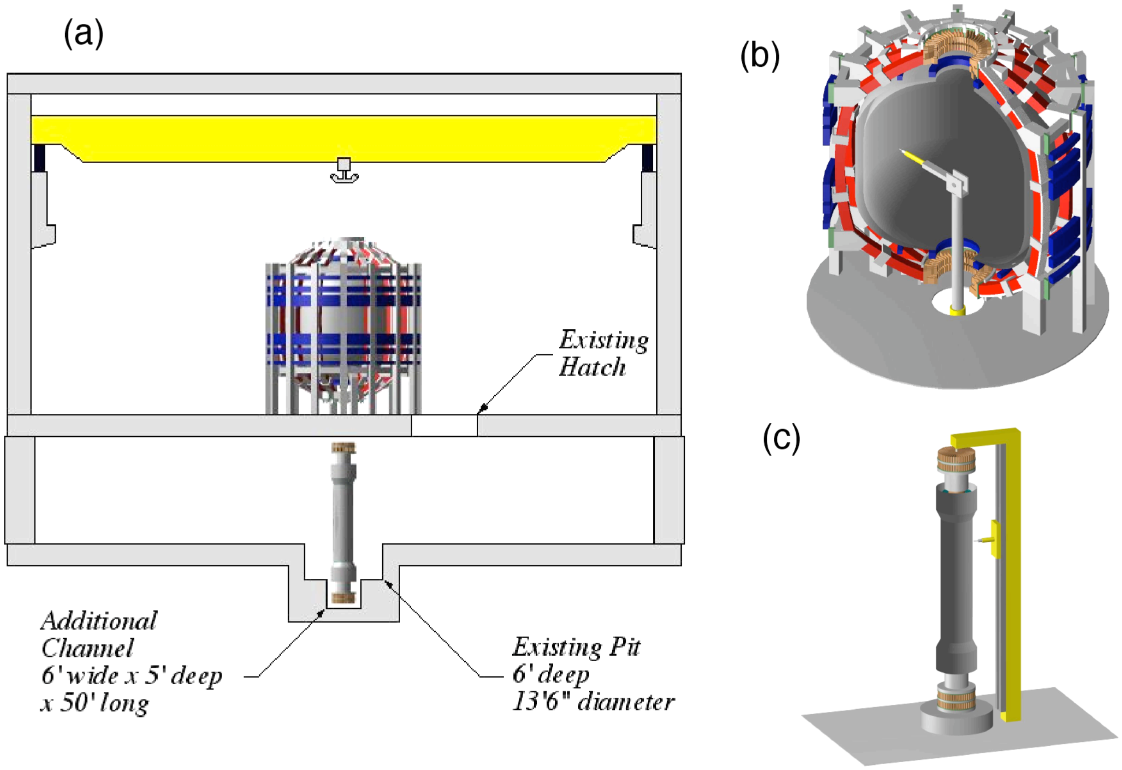

Fig. 13. NSST Remote HandlingSchematics: (a) NSST Center Stack being lowered into the basement for maintenance. (b) A set-up for internal vacuum vessel component maintenance. (c) A set-up for Center-Stack maintenance.

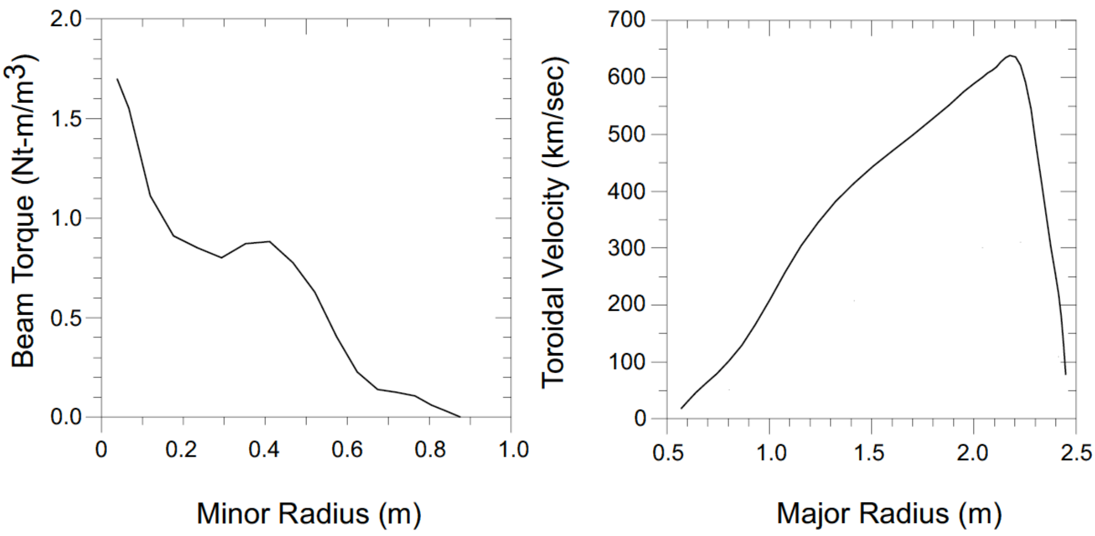

Fig. 14. TRANSP simulation of NBI induced toroidal rotation: (a) Toroidal torque provided by NBI beam. (b) Resulting plasma toroidal rotation profile.

External Distribution

Plasma Research Laboratory, Australian National University, Australia
Professor I.R. Jones, Flinders University, Australia
Professor João Canalle, Instituto de Fisica DEQ/IF - UERJ, Brazil
Mr. Gerson O. Ludwig, Instituto Nacional de Pesquisas, Brazil
Dr. P.H. Sakanaka, Instituto Fisica, Brazil
The Librarian, Culham Laboratory, England
Mrs. S.A. Hutchinson, JET Library, England
Professor M.N. Bussac, Ecole Polytechnique, France
Librarian, Max-Planck-Institut für Plasmaphysik, Germany
Jolan Moldvai, Reports Library, Hungarian Academy of Sciences, Central Research Institute for Physics, Hungary
Dr. P. Kaw, Institute for Plasma Research, India
Ms. P.J. Pathak, Librarian, Institute for Plasma Research, India
Ms. Clelia De Palo, Associazione EURATOM-ENEA, Italy
Dr. G. Grosso, Instituto di Fisica del Plasma, Italy
Librarian, Naka Fusion Research Establishment, JAERI, Japan
Library, Laboratory for Complex Energy Processes, Institute for Advanced Study, Kyoto University, Japan
Research Information Center, National Institute for Fusion Science, Japan
Dr. O. Mitarai, Kyushu Tokai University, Japan
Dr. Jiangang Li, Institute of Plasma Physics, Chinese Academy of Sciences, People's Republic of China
Professor Yuping Huo, School of Physical Science and Technology, People's Republic of China
Library, Academia Sinica, Institute of Plasma Physics, People's Republic of China
Librarian, Institute of Physics, Chinese Academy of Sciences, People's Republic of China
Dr. S. Mirnov, TRINITI, Troitsk, Russian Federation, Russia
Dr. V.S. Strelkov, Kurchatov Institute, Russian Federation, Russia
Professor Peter Lukac, Katedra Fyziky Plazmy MFF UK, Mlynska dolina F-2, Komenskeho Univerzita, SK-842 15 Bratislava, Slovakia
Dr. G.S. Lee, Korea Basic Science Institute, South Korea
Institute for Plasma Research, University of Maryland, USA
Librarian, Fusion Energy Division, Oak Ridge National Laboratory, USA
Librarian, Institute of Fusion Studies, University of Texas, USA
Librarian, Magnetic Fusion Program, Lawrence Livermore National Laboratory, USA
Library, General Atomics, USA
Plasma Physics Group, Fusion Energy Research Program, University of California at San Diego, USA
Plasma Physics Library, Columbia University, USA
Alkesh Punjabi, Center for Fusion Research and Training, Hampton University, USA
Dr. W.M. Stacey, Fusion Research Center, Georgia Institute of Technology, USA
Dr. John Willis, U.S. Department of Energy, Office of Fusion Energy Sciences, USA
Mr. Paul H. Wright, Indianapolis, Indiana, USA

07/07/03

The Princeton Plasma Physics Laboratory is operated
by Princeton University under contract
with the U.S. Department of Energy.

Information Services
Princeton Plasma Physics Laboratory
P.O. Box 451
Princeton, NJ 08543

Phone: 609-243-2750
Fax: 609-243-2751
e-mail: pppl_info@pppl.gov
Internet Address: http://www.pppl.gov